Microbial Ecology (2021) 81:833–846
https://doi.org/10.1007/s00248-020-01666-8

MICROBIOLOGY OF AQUATIC SYSTEMS

Biofilms of *Pseudomonas* and *Lysinibacillus* Marine Strains on High-Density Polyethylene

Maiara Monteiro Oliveira [1,2] · Audrey Menegaz Proenca [1,2] · Eduardo Moreira-Silva [2] · Aline Machado de Castro [3] · Francine Melise dos Santos [1] · Letícia Marconatto [1] · Renata Medina-Silva [1,2]

Received: 29 July 2020 / Accepted: 15 December 2020 / Published online: 3 January 2021

Abstract

Environmental pollution by plastic debris is estimated on a scale of 100 million metric tons, a portion of which is fragmented into micro- and nanoplastics. These fragments are often colonized by bacterial species in marine environments, possibly contributing to the biodegradation of such materials. However, further investigations are necessary to determine the impact of abiotic polymer weathering on biofilm adhesion, as well as the specific biofilm formation strategies employed by marine isolates. Here, we evaluate deep-sea sediment bacterial isolates for biofilm adhesion, extracellular matrix production, and polymer degradation ability. Our study focuses on high-density polyethylene (HDPE) fragments for their high durability and environmental persistence, subjecting fragments to abiotic weathering prior to bacterial colonization. Marine isolates identified as *Pseudomonas* sp. and *Lysinibacillus* sp. exhibited decreasing biofilm formation on weathered HDPE, especially over the first 24 h of incubation. This effect was countered by increased extracellular matrix production, likely improving cell adhesion to surfaces roughened by abiotic degradation. These adhesion strategies were contrasted with a reference *Pseudomonas aeruginosa* strain, which displayed high levels of biofilm formation on non-weathered HDPE and lower extracellular matrix production over the first 24 h of incubation. Furthermore, our results suggest that an increase in biofilm biomass correlated with changes to HDPE structure, indicating that these strains have a potential for biodegradation of plastic fragments. Therefore, this work provides a detailed account of biofilm formation strategies and bacteria-plastic interactions that represent crucial steps in the biodegradation of plastic fragments in marine environments.

Keywords Bacteria · Microplastics · Aquatic organisms · Environmental microbiology

Introduction

In 2016, global plastic production reached 396 million metric tons, of which roughly 100 million metric tons are classified as terrestrial or marine pollutants [1]. The critical increase in production, consumption, and improper disposal of synthetic plastic polymers has culminated in a dramatic human impact on ecosystems [2]. This plastic waste spreads in the environment as visible fragments (≥ 5 mm), microplastics (< 5 mm), or nanoplastics (< 0.1 μm) [3], all offering stable surfaces for the colonization by diverse microbial species [4] and also for biofilm attachment [5]. Biofilms consist of microbial communities that adhere to solid surfaces and produce an extracellular matrix in which they remain embedded, representing the most common growth state for many microbial species, such as *Pseudomonas* sp. and *Candida albicans* [6, 7]. Biofilms attached to floating and buried plastic waste may result in higher concentrations of microbial life (including pathogens) than natural surfaces since they provide a more stable, undegradable surface on which microbes may efficiently attach and reproduce [3, 8]. Nonetheless, there are

✉ Renata Medina-Silva
renata.medina@pucrs.br

[1] Geobiology Laboratory, Institute of Petroleum and Natural Resources, Pontifical Catholic University of Rio Grande do Sul, PUCRS, Av. Ipiranga 6681, Building 96J, Porto Alegre, RS 90619-900, Brazil

[2] Immunology and Microbiology Laboratory, School of Health and Life Sciences, Pontifical Catholic University of Rio Grande do Sul, PUCRS, Av. Ipiranga 6681, Building 11, Porto Alegre, RS 90619-900, Brazil

[3] Biotechnology Division, Research and Development Center (CENPES), PETROBRAS, Av. Horácio Macedo 950, Rio de Janeiro, RJ 21941-915, Brazil

crucial gaps in our knowledge regarding the mechanics of biofilm formation on plastic residues by environmental microbes.

Among the most recalcitrant plastic pollutants, the thermoplastic polyethylene (PE), constituted by the chain $(CH_2\text{-}CH_2)_n$, represents a challenge for biodegradation. Its versatile nature has resulted in wide industrial applications, often in the form classified as high-density polyethylene (HDPE) for its high strength-to-density ratio and strong intramolecular forces [9]. HDPE is characterized by > 90% crystallinity, low chemical reactivity, and resistance to stress, compression, and tension. Whether synthetized from a petrochemical base or plant biomass [9], the polymer retains its stability properties [10], requiring over 100 years for soil mineralization [11, 12]. Along this slow weathering process, HDPE fragments represent potential biofilm attachment surfaces in natural environments.

Due to intense and permanent deposition of plastic waste, marine environments, especially in high depths [13–16], become a target for bioprospection of microorganisms with potential for adhesion and degradation of thermoplastic resins [17–20]. However, the biofilm formation mechanisms on plastic surfaces of microbial isolates from these environments are not entirely elucidated [21]. Here, we evaluate deep-sea bacterial isolates for their biofilm attachment and structure on HDPE following a gradient of weathering treatments. We demonstrate that *Pseudomonas* sp. and *Lysinibacillus* sp. strains exhibited a decreasing early (first 24 h) biofilm attachment with HDPE weathering, while increasing the production of extracellular matrix to favor rougher surface adhesion. The formation of biofilms on HDPE surfaces also resulted in changes to the chemical structure of the polymer, thus suggesting the potential involvement of these strains in the biodegradation of plastic pollutants.

Material and Methods

Origin of Bacterial Isolates

Deep-sea sediment samples were collected in 2013 from the Pelotas Basin (Brazil), a methane cold seep site [22] with the occurrence of a methane-based chemosynthetic metazoan community [23]. Bacterial strains were previously isolated from sediment samples obtained at 0 to 3 m below surface with a piston core, at a site with ~ 1.500 m water column. Micro- and nanoplastic fragments were detected in these sediment samples when observed under optic microscopy (from 100 to 1000× magnification) (unpublished data). For bacterial isolation, samples were inoculated and spread in nitrate mineral salts (NMS) broth and agar, respectively, with methane as the sole carbon source. Cultures of all microbial isolates were kept stored at − 80 °C with 5% dimethyl sulfoxide (DMSO) at 30% (v/v).

Biochemical profiles previously obtained (unpublished data) were used as parameters to select five bacterial isolates that were used for the experiments of biofilm formation. Isolates M1, M2, and M3 were obtained from 0-m (seabed) samples, M4 from 1.5 m, and M5 from 3-m-deep sediment samples. The selected isolates were recovered from stocks by cultivation in brain heart infusion (BHI) broth, at 28 °C, for 12–24 h. Isolates were further characterized by Gram staining under optical microscopy (1000×), to confirm their morphology and culture purity. In addition, *Pseudomonas aeruginosa* ATCC 27853 strain, described as biofilm producer on polystyrene [24], was used as a reference strain for all experiments. All strains were cultured and maintained in tryptic soy agar (TSA) medium and incubated overnight at 25 °C, to be later used in biofilm formation experiments.

Taxonomic Identification of Bacterial Strains

For taxonomic identification of isolates, DNA was extracted using the QIAamp® DNA Stool Mini Kit (50) (Qiagen). The complete sequence of small ribosomal subunit rRNA (16S) gene was amplified through polymerase chain reaction (PCR) using the following primers: 9 forward (5′ AGA GTT TGA TCC TGG CTC AG 3′) and 1542 reverse (5′ AGA AAG GAG GTG ATC CAG CC 3′) [25]. Amplification was performed in a 50 μL mixture, consisting of 1.5 mM $MgCl_2$, 0.2 μM of each primer, 0.2 mM of each dNTP, 1 U Platinum *Taq* DNA polymerase, 1X PCR reaction buffer, and approximately 10 ng of genomic DNA. PCR conditions used were the following: an initial activation at 94 °C for 2 min and 25 cycles of 45 s at 94 °C, 45 s of 55 °C, and 60 s at 72 °C, followed by an extension at 72 °C for 3 min. The reaction products were purified using Wizard® SV Gel and PCR Clean-Up System (Promega) and sequenced by the capillary method by Myleus Facility Company (Belo Horizonte, Minas Gerais, Brazil). The forward and reverse sequencing reads were assembled and trimmed into single contigs using the software DNA Sequence Assembler version 5.15.0 (Phred quality score cutoff of < 20). After assembly, 16S rRNA sequences were deposited in the NCBI database: M1 (MT074711), M2 (MT074712), M3 (MT074713), M4 (MT074714), and M5 (MT074715). Contigs were then aligned against the NCBI database through the Basic Local Alignment Search Tool (BLAST). Similar and reference sequences were downloaded from the National Center for Biotechnology Information (NCBI) database to perform a phylogenetic analysis. Sequences were further aligned using the ClustalW tool incorporated in MEGA X. Phylogenetic analyses were performed using the Phylogeny Tool on MEGA X [26]. Then, the phylogenetic trees were constructed using the maximum likelihood method and the Tamura-Nei

model [27]. Statistical significance was measured by 1000 bootstrap replications.

HDPE Fragments and Accelerated Weathering

HDPE pellets used in this study are from a sugarcane source donated by Indústria Petroquímica Braskem S.A. A total of 2 g HDPE pellets were pressed between Teflon-coated steel plates at 130 °C, applying a 3-ton load for 2 min from a MA098/C hydraulic press (Marconi), obtaining large films (10–15 cm). Accelerated weathering of HDPE large films was performed using a QUV Accelerated Weathering Tester (QUV/Spray/240, Q-Lab) that simulates the weathering process causing damage on polymers occasioned by UV irradiation, humidity, and dew [28]. In this work, the conditions used were based on ASTM G154 – 12 a protocol: 8 h at 60 °C UVA radiation (340-nm UV radiation lamp with an incidence of 90°) and 4 h at 40 °C condensation with drinking water (50% relative humidity). The accelerated weathering treatments were performed for 400 h, 600 h, and 800 h and named in this work as 400-HDPE, 600-HDPE, and 800-HDPE, respectively. All large films were then manually fragmented into small fragments of 5 mm, which were used in the following assays.

Biofilm Formation Assay on HDPE

HDPE fragments were disinfected through an immersion washing procedure with 70% ethanol for 30 min, followed by sterile ultrapure water washing [29]. Washed fragments were dried at room temperature within a laminar flow chamber [5]. The protocol for the biofilm formation assay did not use a biofilm induction step, to analyze the spontaneous formation ability of marine strains. Bacterial colonies from TSA medium were used to prepare a pre-inoculum in a 4-mL tryptic soy broth (TSB) medium, followed by incubation overnight at 25 °C. After, 100 μL of these cultures was transferred to a 10-mL sterile TSB broth in Erlenmeyer flasks. With an optical density (OD_{600}) around 1 A.U., 1 μL inoculum and one HDPE fragment were added to 15 mL TSB in Erlenmeyer flasks. These cultures were incubated for 24 or 48 h at 25 °C under a static condition (adapted from [30]), The HDPE fragments from these cultures were then prepared for different analysis, as described below.

Crystal Violet Assay

After interaction with bacterial cells, HDPE fragments were aseptically recovered from Erlenmeyer flasks, transferred to 2-mL microtubes, and rinsed with sterile ultrapure water, in order to remove planktonic cells or those that were weakly attached to their surface. Subsequently, 2 mL of 0.25% crystal violet was added to each microtube and the system was incubated at 25 °C for 30 min. The microtubes were washed with sterile ultrapure water and dried at room temperature, within a laminar flow chamber, for 10 min. The crystal violet dye bound to the biofilm was solubilized with 660 μL of 70% ethanol and incubated at 25 °C for 30 min. Dye absorbance was measured at 595 nm using SpectraMax 190 Microplate Reader (Molecular Devices) (adapted from [30]). According to the average of nine optical densities obtained (ODi), which was compared to the optical density of the negative control (ODc), all isolates were classified into four categories based on the following criteria: if $ODi \leq ODc$ (non-adherent), if $ODc < ODi \leq 2 \times ODc$ (weakly adherent), if $2 \times ODc < ODi \leq 4 \times ODc$ (moderately adherent), or if $4 \times ODc < ODi$ (strongly adherent) [31].

Scanning Electron Microscopy

After the biofilm formation assay, HDPE fragments were fixed with 2.5% glutaraldehyde and washed with 0.1 M phosphate buffer. Then, fragments were subjected to dehydration with increasing ethanol concentrations (50–100%) and finally metallized with gold (BAL-TEC– SCD 050 – Sputter Coater, Balzers, Liechtenstein). A secondary electron detector at 20.0 kV (Scanning Electron Microscopy, INSPECT-F50, FEI Company Inspect, Eindhoven, Netherlands) was used to analyze and obtain the images at the Central Laboratory of Microscopy and Microanalysis (LabCEMM) from Pontifical Catholic University of Rio Grande do Sul (PUCRS).

Atomic Force Microscopy

After interaction with bacterial cells, HDPE fragments were fixed with 2.5% glutaraldehyde and washed with sterile ultrapure water and dried at room temperature. For atomic force microscopy analysis at the LabCEMM from PUCRS, a Bruker Dimension Icon PT equipped with an OCR 8-10 5A probe (71-kHz resonant frequency, 0.73 N/m spring constancy, 100 μm length, and 40 μm width) with a resolution of 256 × 256 pixels was used. Using NanoScope Analysis Software (version 1.50), the height sensor mode determined the average HDPE surface roughness value. The greater the roughness of the analyzed surface, the greater heterogeneity, which is mainly characterized by the square root of the arithmetic mean of the vertical deviation from a reference line (Rq parameter) [32, 33].

Fourier-Transform Infrared Spectroscopy

After biofilm formation, HDPE films were washed with sterile ultrapure water and dried at room temperature. A PerkinElmer Spectrum 65 FTIR Spectrometer with attenuated total reflectance (ATR) accessory was used to collect spectra from 650 to 4000 cm^{-1}. The resolution was set at 4 cm^{-1}. The ATR

diamond crystal was cleaned with acetone and a background scan was performed between each sample. Samples were compressed against the diamond with a force of 30 N to guarantee the contact between ATR crystal and sample, with no damage in HDPE fragments. A peak height algorithm of Perkin Elmer Spectrum Software was used to identify absorption bands, obtaining spectra of HDPE fragments, which were compared to absorption bands reported in the literature. Each spectrum was pre-processed by subtracting a polynomial fit baseline and vector-normalizing absorbance values.

For the quantification of non-colonized HDPE fragments, the carbonyl index was calculated according to the specified area under the band method described by Almond et al. [34]. The crystallinity of HDPE fragments was estimated as described by Zerbi et al. [35], using the peaks at 1464 and 1474 cm^{-1} as indicators of the amorphous and crystalline phase, respectively. In this method, the percentage of amorphous content is estimated by the following equation:

$$X = \frac{\frac{1-I_a/I_b}{1.233}}{1+I_a/I_b} \text{ x } (100)$$

where I_a represents the absorbance of the crystalline peak (1474 cm^{-1}), I_b represents the absorbance of the amorphous peak (1464 cm^{-1}), and 1.233 is a constant representing fully crystalline HDPE. From the percentage of amorphous content (X), the percentage of crystalline content is given as 100–X.

For the analysis of biofilm-colonized HDPE, spectra of non-colonized HDPE fragments were used as negative controls, allowing for the subtraction of HDPE bands from all biofilm spectra. The comparison of biofilm polysaccharide levels was performed as a function of biofilm biomass, through the normalization of absorbance values by the amide II peak.

Statistical Analysis

Biofilm formation data from crystal violet assay (CVA) analyses were expressed as mean ± SEM, normalized in relation to negative controls, and were obtained from a triplicate of the assay. The Kolmogorov–Smirnov test was applied to verify a normal data distribution for CVA values. Differences among samples obtained from CVA were analyzed by variance with two-way ANOVA, followed by Tukey's test. Moreover, Fourier-transform infrared spectroscopy (FTIR) data were normalized. Differences among spectra obtained from FTIR were analyzed by the Friedman test, followed by Dunn's test. Statistical analyses were performed using R (version 3.6.1), with p values < 0.05 considered significant.

Results

Taxonomic Identification of Bacterial Strains

To investigate marine bacteria for their biofilm formation ability on plastic fragments, we selected five isolates obtained from deep-sea sediment. We identified these strains through 16S rRNA gene sequencing, which is presented in a phylogenetic analysis (Fig. 1). Isolates M2, M3, and M5 exhibited high similarity with *Pseudomonas* sp. in the phylogeny. Although they showed to be related to the species *P. rhodesiae* (*Pseudomonas fluorescens* group), these strains formed a separate branch, being more closely related to each other than to these reference *Pseudomonas* sequences. Isolate M1 was identified as *Stenotrophomonas* sp., indicating a close relationship with a strain from the species *S. rhizophila*. The M4 strain was identified as *Lysinibacillus* sp., which clustered with the representative strain of the species *Lysinibacillus fusiformis* in the phylogenetic tree. All these five isolates were used in initial biofilm experiments to verify their efficiency in biofilm formation.

Evaluation of Biofilm Adhesion

To determine the capacity of marine isolates to colonize HDPE surfaces, we performed a CVA colorimetric analysis. We evaluated the intensity of biofilm formation after 24 or 48 h of culturing, using these experiments to select the most efficient biofilm-producing strains (Fig. 2a). A *Pseudomonas aeruginosa* strain (ATCC 27853) was used as a reference for its high biofilm formation ability. After 24 h of incubation with HDPE, the strains exhibited significant differences in their levels of biofilm attachment (one-way ANOVA, $F = 22.75$, $p < 0.001$). A post hoc analysis revealed that the reference strain performed better than marine isolates (Tukey's HSD, $p < 0.05$), while strains M1 and M2 were the least efficient biofilm-forming isolates ($p < 0.001$). After 48 h, all strains performed similarly (one-way ANOVA, $F = 1.57$, $p = 0.18$). These observations prompted the selection of isolates M3, M4, and M5 for further experiments.

Since HDPE is subject to intense weathering in natural environments, which might offer an improved attachment surface for bacterial biofilms, we exposed HDPE fragments to an accelerated weathering treatment. This process induced UV, temperature, and humidity damage for 400, 600, and 800 h. Surprisingly, our results showed a decrease in biofilm attachment with surface weathering at 24 h (Fig. 2b; one-way ANOVA, $F = 113.5$, $p < 0.001$). While non-weathered HDPE offered the best attachment surface, an equally low level of biofilm formation was detected on 600- and 800-HDPE (Tukey's HSD, $p = 0.998$). This overall trend was observed for all strains (Fig. 2c; two-way repeated-measures ANOVA, $F = 70.915$, $p < 0.001$), although the isolates

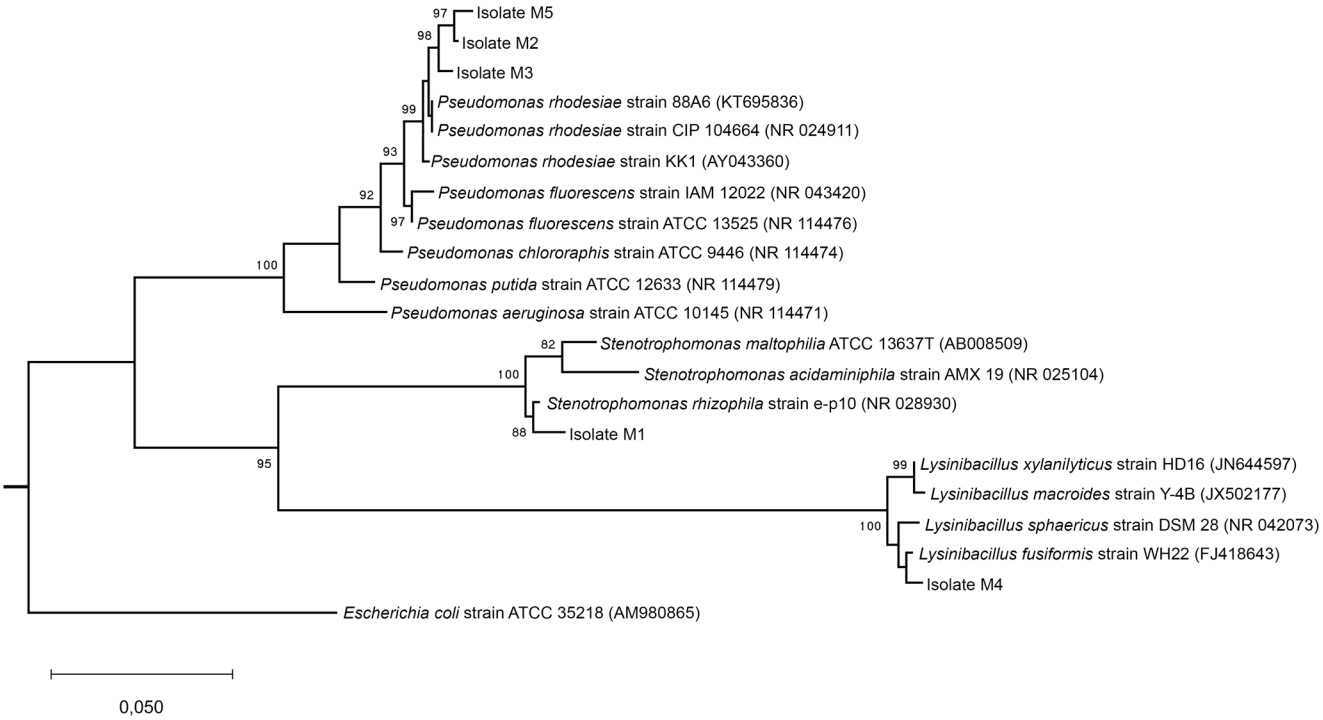

Fig. 1 Taxonomic identification of bacterial isolates M1, M2, M3, M4, and M5. Phylogenetic analyses were performed with reference sequences obtained from the Genbank database. Phylogenetic trees were constructed using the maximum likelihood method and Tamura-Nei model based on 16S rRNA gene sequences. Bootstrap percentages based on 1000 replications are shown at branch points (values bellow 80 were cutoff)

differed in their response to the treatment ($F = 44.828$, $p < 0.001$). For instance, the reference strain showed the highest biofilm adhesion for all weathering levels, while M3 and M4 exhibited nearly identical attachment (two-way repeated-measures ANOVA; HDPE age: $p < 0.001$, strain: $p = 0.131$).

A similar effect of HDPE weathering was observed on 48-h experiments (Fig. 2d; one-way ANOVA, $F = 11.13$; $p = 0.001$), with bacteria showing the least attachment to 600- and 800-HDPE. Although biofilm formation decreased for all strains (Fig. 2e; two-way repeated-measures ANOVA, $F = 13.808$, $p < 0.001$), there was strong variation in the response of each isolate to surface weathering ($F = 16.109$, $p < 0.001$; strain-weathering treatment interaction: $F = 22.878$, $p < 0.001$). Isolate M5 exhibited high attachment to non-weathered, 400- and 600-HDPE, surpassing the reference strain in the latter treatment (Fig. 2e). Strains M3 and M4 again showed similar biofilm formation levels ($F = 0.011$, $p = 0.916$), despite their overall attachment decreasing with surface weathering ($F = 10.437$, $p < 0.001$). Taken together, these results indicate that HDPE weathering hinders biofilm adhesion, with a stronger effect observed for 24-h experiments.

To further investigate biofilm adhesion efficiency, we compared the response of each strain to weathering after 24 and 48 h of incubation (Fig. S1). While the reference strain had a significantly higher adhesion ability in 24 h comparing to 48 h ($F = 126.071$, $p < 0.001$) independently of the surface weathering (Fig. S1a), this effect was not observed for all marine isolates. M3 exhibited only a slightly improved attachment at 24 h ($F = 34.494$, $p < 0.001$), but no significant distinction was observed for M4 ($F = 1.736$, $p = 0.192$) and M5 ($F = 2.920$, $p = 0.092$). This pattern could be explained by the domestication of our reference strain for fast growth in laboratory conditions, favoring early attachment. Marine strains, on the other hand, experience longer time scales in the natural environment. Therefore, albeit showing overall lower biofilm formation, marine isolates are equally efficient after 24 and 48 h, with isolate M5 surpassing the reference strain after 48 h in weathered HDPE.

Morphological Aspects of Biofilm Attachment

To evaluate the morphological interaction of bacterial biofilms with HDPE polymers, we analyzed the isolates through scanning electron microscopy (SEM). To illustrate this analysis, we selected images that were representatives of others within the same sample. These images, shown in Fig. 3, corroborated the biofilm formation ability of *Pseudomonas* sp.—M3 and M5—and *Lysinibacillus* sp.—M4—on HDPE fragments. Following the previous trend, surface weathering seemed to have a negative impact on biofilm attachment. M3 and M5 exhibited a tendency of efficient attachment to non-weathered HDPE after 24 h of incubation, confirming observations reported in Fig. S1b and d. After 48 h of incubation, surface weathering seemed to induce a decrease in biofilm

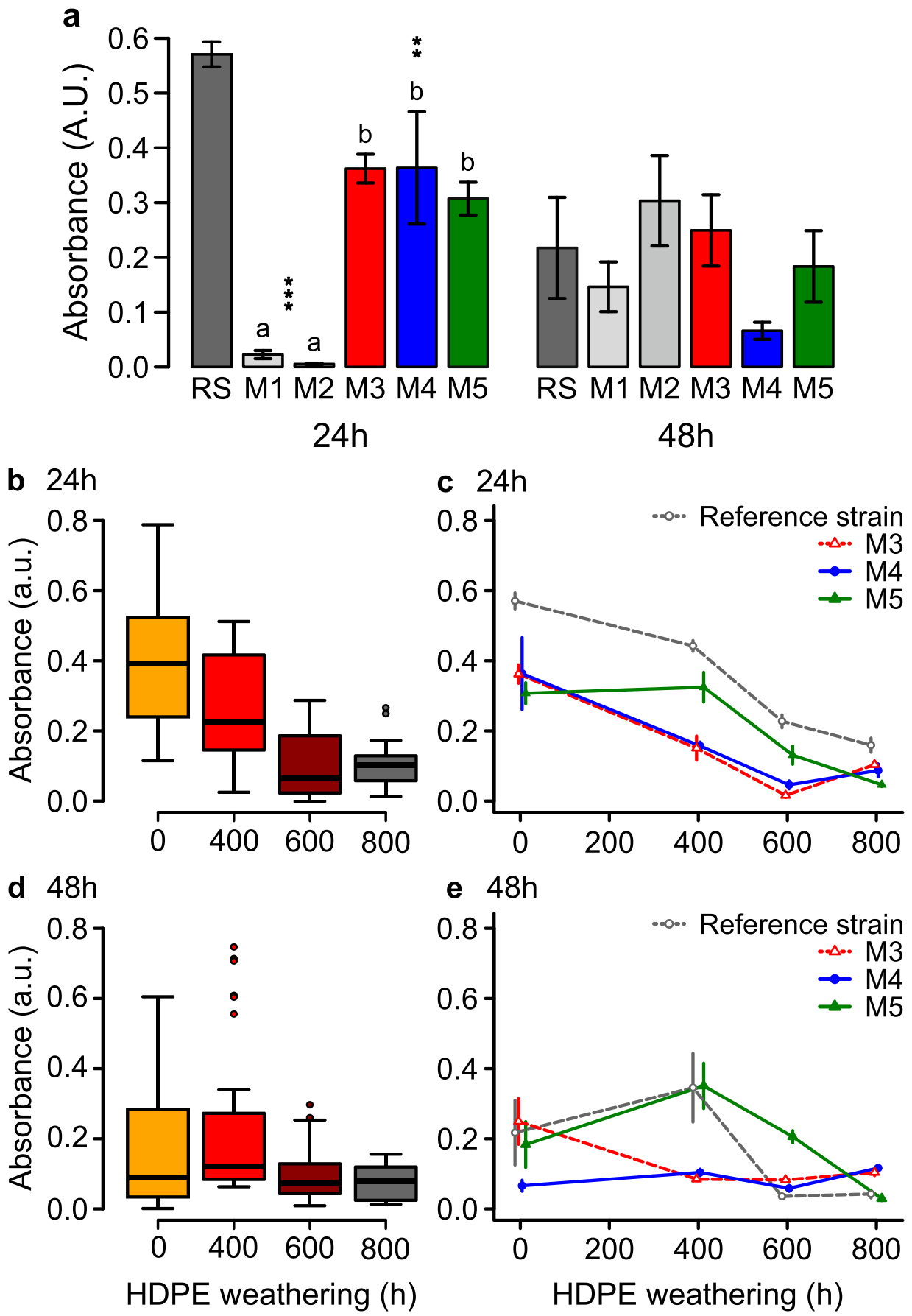
a
Absorbance (A.U.)
0.6
0.5
0.4
0.3
0.2
0.1
0.0
a
a
b
b
b
***
**
RS M1 M2 M3 M4 M5
RS M1 M2 M3 M4 M5
24h
48h
b 24h
Absorbance (a.u.)
0.8
0.6
0.4
0.2
0.0
0 400 600 800
c 24h
Reference strain
M3
M4
M5
0 200 400 600 800
d 48h
Absorbance (a.u.)
0 400 600 800
HDPE weathering (h)
e 48h
Reference strain
M3
M4
M5
0 200 400 600 800
HDPE weathering (h)

◀ **Fig. 2** Biofilm formation on non-weathered and weathered HDPE surfaces, quantified by CVA absorbance. **a** Marine strains M3, M4, and M5 showed similar levels of biofilm formation after 24 h of incubation with non-weathered HDPE. Letters **a** and **b** represent grouping indicated by Tukey's test, with $p < 0.01$ (**) and $p < 0.001$ (***). No differences between strains were observed in 48-h experiments. **b** and **d** boxplots represent CVA absorbance for M3, M4, M5, and the reference strain for all weathering treatments (indicated by colors and labels). Horizontal bar indicated median; box boundaries indicate 25th and 75th percentiles. **b** Biofilm formation decreased with HDPE weathering in 24-h experiments. **c** This negative correlation was observed for all strains. **d** For 48-h experiments, HDPE weathering had a smaller effect on biofilm formation. **e** Isolates M3 and M4 showed low biofilm adhesion, while M5 biofilm formation decreased on HDPE weathered for over 400 h

attachment for the reference strain when compared to the marine isolates (Fig. 3), which is in line with the sharper decrease in biofilm formation data (Fig. 2e). In 800-HDPE, we did not observe any cells of the reference strain and it was possible to detect alterations of the HDPE structure due to the 800 h weathering (Fig. 3). Contrary to our previous assay, however, the reference strain seemingly increased attachment with surface weathering in 24-h experiments.

As a specific characteristic of biofilm attachment, our microscopy analysis also detected the presence of extracellular components surrounding the bacterial cells, which we inferred as polymeric substances of an extracellular matrix (EM). The EM was observed in some biofilms, including those of the marine isolates (Fig. 3). The presence of EM in the biofilms could indicate that marine isolates may devote part of their resources toward biofilm structuring, possibly at the cost of slower colonization. For these strains, the proportion of EM within the biofilm seemed to increase with HDPE weathering, which could be a response to the increased heterogeneity of weathered surfaces. Finally, we observed a tendency of high levels of EM synthesis on 48-h experiments for all marine strains, suggesting that the synthesis of its components may develop over a longer timescale after the initial biofilm colonization phase.

In addition, some cells within some biofilms were linked to each other by appendages structures. Shorter and longer appendages, that resemble a different kind of *pili*, were observed between cells and HDPE fragments (Fig. 4). We did not investigate which type of appendages they may be, even so, these structures are indicative of mature biofilms, which may favor cellular communication and improve biofilm adhesion to the polymer surface [36].

Topographic Extracellular Matrix Quantification

To determine the heterogeneity of biofilm surfaces on HDPE fragments, we performed AFM three-dimensional topography measurements (Table 1). The biofilms that displayed higher heterogeneity are shown in Fig. S2. Despite the trend of increasing surface roughness due to weathering (negative controls, Table 1), marine strains incubated for 24 h produced a more homogeneous biofilm topography on 600- and 800-HDPE (one-way ANOVA, $F = 6.073$, $p = 0.033$). After 48 h, marine strain biofilms exhibited similar roughness independently of the substrate weathering level ($F = 0.188$, $p = 0.674$). These results could indicate that biofilm coverage and potential EM production compensated for the substrate roughness produced by weathering.

Chemical Structure of HDPE Fragments and Biofilms

To investigate changes to the chemical structure of HDPE fragments, we analyzed ATR-FTIR spectra of all strains and substrate weathering conditions (Fig. S3). HDPE fragments not exposed to bacterial colonization were examined first as a negative control (Fig. 5). For all weathering treatments, the most prominent peaks in all spectra corresponded to characteristic HDPE bands (Fig. 5a and b), assigned as C–H stretch (2915 cm^{-1} and 2848 cm^{-1}), CH_2 bend (1473 cm^{-1} and 1462 cm^{-1}), and CH_2 rock (730 cm^{-1} and 719 cm^{-1}) [37]. No shifts or significant changes in absorbance were observed for these peaks. However, two new peaks appeared in weathered fragments at 909 and 1177 cm^{-1} (Fig. 5a and b), which could be related to chain branching and chain breaking, respectively. Weathered HDPE fragments also displayed bands suggesting the formation of carbonyl groups (e.g., 1715 cm^{-1}) due to abiotic oxidation [38]. To quantify this oxidative process, we calculated the carbonyl index using the "specified area under band" method [34], dividing the carbonyl area (1420 to 1500 cm^{-1}) by the polymer reference area (1650 to 1850 cm^{-1}) as indicated in Fig. 5a and b. The results are presented in Fig. 5c, indicating a sharp increase in carbonyl groups with HDPE weathering. Finally, we investigated whether accelerated weathering impacted the crystalline content of HDPE fragments (see Material and Methods for details), but no changes were observed (Fig. 5d).

Once the chemical and structural characteristics of weathered HDPE fragments were described, we used ATR-FTIR to determine whether biofilm colonization impacted these characteristics. Using the amide II band area (1500–1600 cm^{-1}, C–N bend and N–H stretch in proteins) as a proxy for biofilm biomass [36], we observed a negative correlation between biofilm formation and the HDPE C–H stretch absorbance (Fig. 6a; $a = -0.036$, $R^2 = 0.654$, $p < 0.001$), represented by the peak at 2915 cm^{-1}. To further investigate this pattern, we subtracted the background spectra of non-colonized HDPE from the spectra of biofilm-colonized fragments, thus focusing on the spectral changes produced by bacterial strains. From this analysis, we observed that biofilm colonization produced both a decrease of C–H stretch and an increase of CH_2 bend absorbance (Fig. 6b; $a = -1.581$; $R^2 = 0.164$; $p = 0.012$).

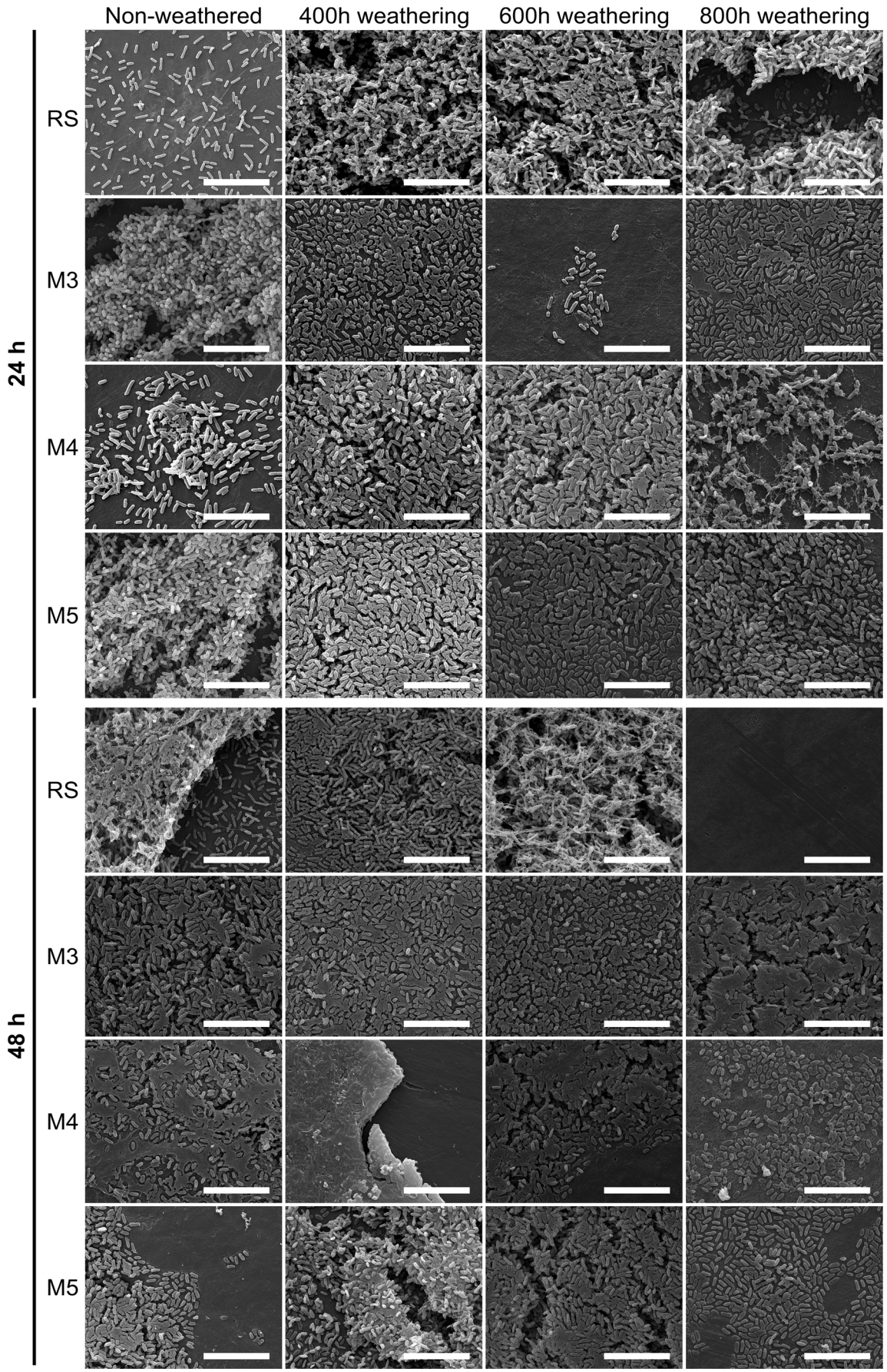
Non-weathered
400h weathering
600h weathering
800h weathering
24 h
48 h
RS
M3
M4
M5
RS
M3
M4
M5

◀ **Fig. 3** SEM imaging of bacterial biofilms on HDPE surfaces. The images show biofilm adhesion of the reference strain (RS) and marine isolates (M3, M4, M5) on non-weathered and weathered HDPE surfaces for 24 h and 48 h. Magnification = 10,000×. Scale bars = 10 μm

ATR-FTIR spectra also allowed us to investigate the production of EM by each strain. We normalized each spectrum by the amide II peak and calculated the area of the spectral region corresponding to carbohydrates (900–1150 cm^{-1}), obtaining an estimate of EM relative to biofilm biomass. For 24-h experiments, we observed that all marine strains produced more EM than the reference strain (Fig. 6c), with M3 producing the highest EM level on 600-HDPE. For 48-h experiments, the reference strain exhibited high EM production on non-weathered HDPE, while marine strains showed higher EM levels on 600-HDPE (Fig. 6d). Taken together, these results suggest that bacterial adhesion resulted in the formation of biofilms with EM synthesis, with different levels of EM production in marine strains comparing to the reference strain, which seemed to be related to the chemical structure of plastic fragments.

Table 1 Values of HDPE roughness (nm) of negative control, reference strain, and marine isolates, after biofilm formation assays, obtained by AFM and analyzed by NanoScope Analysis Software (version 1.50) through height sensor mode

Samples	Roughness (nm)							
	Non-aged		400 h		600 h		800 h	
	24 h	48 h	24 h	48 h	24 h	48 h	24 h	48 h
Negative control	35	35	64.2	68.4	47.3	79.1	35	56.6
Reference strain	74.7	86	97.2	75	125	94.7	103	117
M3	111	157	112	84.4	71.6	88.5	116	60.7
M4	95.1	35.2	111	116	89.8	185	62	104
M5	172	81.1	139	92.6	90.8	92.3	60.6	125

Discussion

Plastic waste is constantly deposited in marine environments, especially in deep-sea layers [13–15], including seabed sediments [16]. In this context, deep-sea sediment represents a target for microorganisms capable of adhering to polymer surfaces [17–20]. The microbial communities in these "plastispheres" contain heterotrophic, autotrophic, predators, and symbiont microorganisms [3, 20], with an ecological impact ranging from local food chains to oceanic biogeochemical cycles [29, 39]. Because such microbes could also contribute to the degradation of plastic waste, our study evaluated bacterial isolates from deep-sea sediment for their biofilm formation ability. Particularly, we focused on HDPE plastic

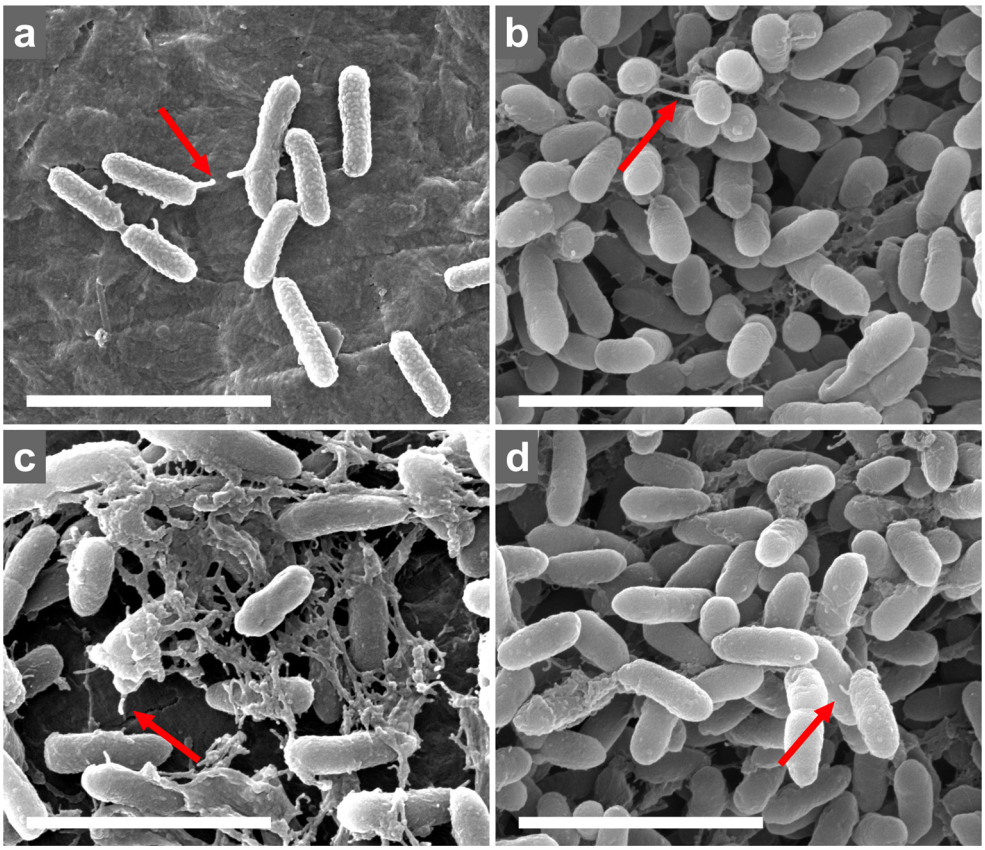

Fig. 4 Appendage-like bacterial structures (arrows), which were observed mainly in 24-h biofilms on non-weathered HDPE. **a** Reference strain, **b** M3, **c** M4, and **d** M5 isolates. SEM imaging. Magnification = 50.000×. Scale bars = 3 μm

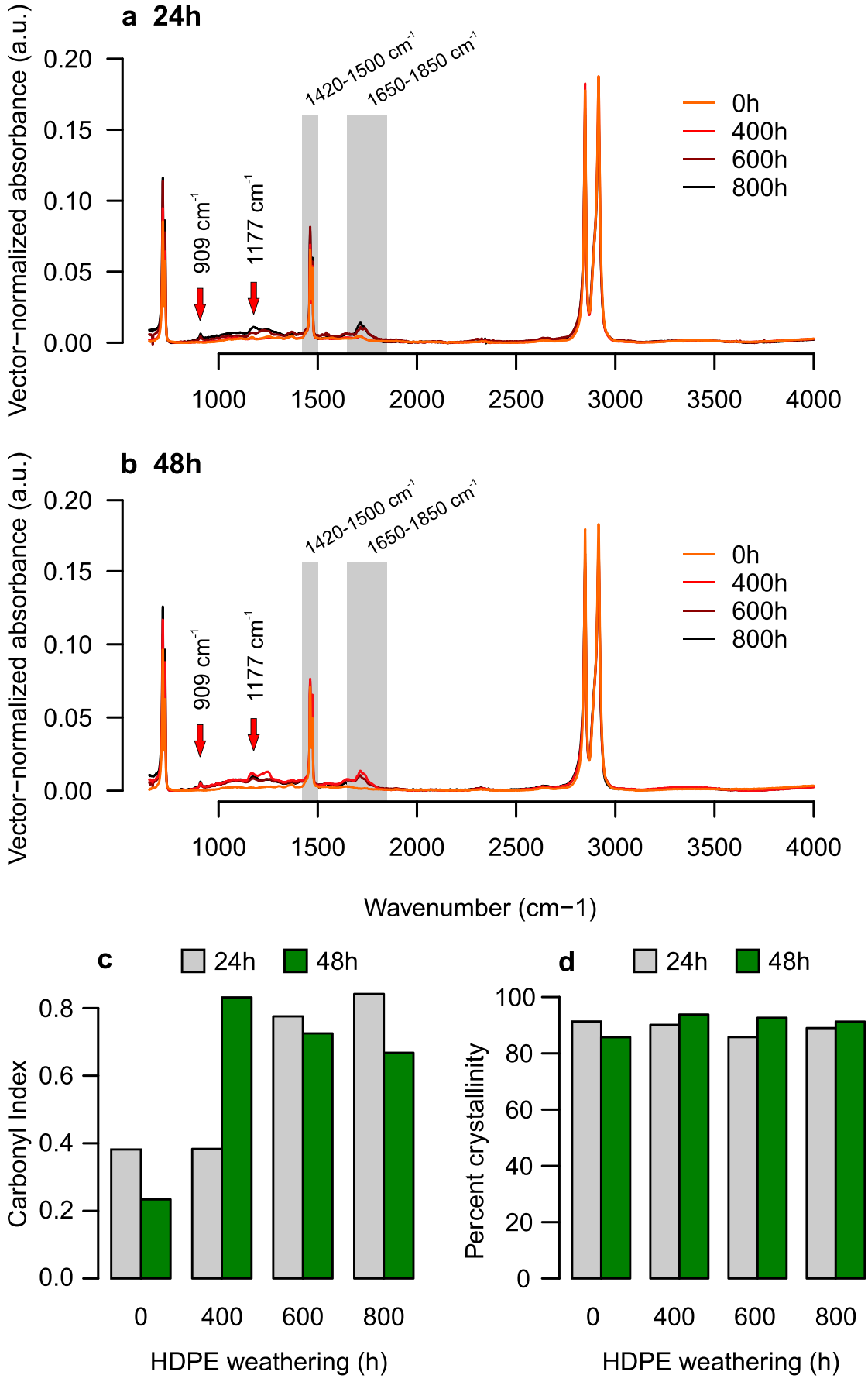
a 24h
b 48h
Vector−normalized absorbance (a.u.)
0.20
0.15
0.10
0.05
0.00
1420-1500 cm-1
1650-1850 cm-1
909 cm-1
1177 cm-1
0h
400h
600h
800h
1000
1500
2000
2500
3000
3500
4000
Wavenumber (cm−1)
c
24h
48h
Carbonyl Index
0.8
0.6
0.4
0.2
0.0
0
400
600
800
HDPE weathering (h)
d
Percent crystallinity
100
80
60
40
20
0

◀ **Fig. 5** ATR-FTIR analysis of non-colonized HDPE fragments subjected to accelerated weathering. **a** and **b** Vector-normalized HDPE spectra show the characteristic HDPE peaks at 719, 730, 1462, 1473, 2848, and 2915 cm^{-1} for both 24 h (**a**) and 48 h (**b**) experiments. The area highlighted in gray was used for the determination of the carbonyl index in **c**, with the spectral area 1650–1850 cm^{-1} representing the carbonyl groups and 1420–1500 cm^{-1} providing the HDPE reference. **c** Estimate of the carbonyl index, showing an increase in oxidized components with weathering. **d** Percent crystallinity of HDPE fragments as determined by the ratio between the amorphous peak (1462 cm^{-1}) and the crystalline peak (1473 cm^{-1}) as described in the Material and Methods section

fragments for their low degradability and broad industrial use—thus representing a recurring pollutant.

Through a pre-treatment inducing thermal and photo-oxidation, we reenacted the natural weathering of thermoplastic resins in the environment [11, 38], determining the impact of abiotic degradation on microbial attachment and biofilm formation [3, 38]. Weathering resulted in increased surface roughness, leading to an overall decrease of biofilm attachment (Fig. 2b). Compared to the *P. aeruginosa* reference strain, the marine *Pseudomonas* sp. and

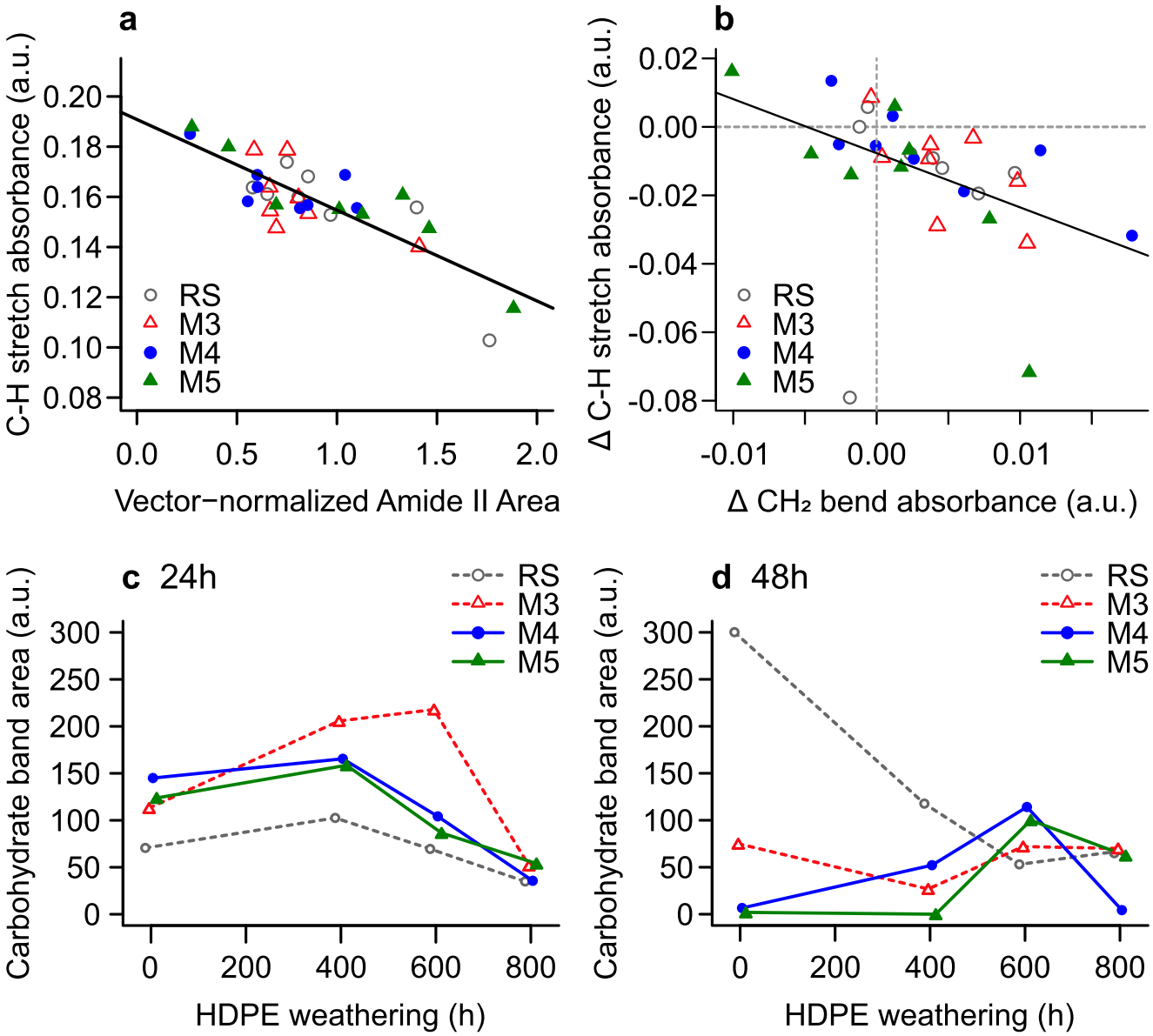

Fig. 6 ATR-FTIR analysis of HDPE structure changes and EM production by bacterial biofilms. **a** and **b** Data extracted from vector-normalized spectra. **a** The HDPE band at 2915 cm^{-1}, assigned as C–H stretch, showed decreasing absorbance for increased biofilm biomass, indicated by the area of the amide II spectral region. **b** The difference in absorbance between colonized and non-colonized HDPE fragments showed a negative correlation between C–H stretch and CH_2 bend regions. **c** and **d** Amide-normalized spectra were used to calculate the area of the carbohydrate spectral region (900–1150 cm^{-1}), representing EM production relative to biofilm biomass for 24 h (**c**) and 48 h (**d**) experiments. RS, reference strain

Lysinibacillus sp. isolates exhibited lower attachment levels in the first 24 h (Fig. 2c), with an observed tendency to respond to weathering through increased production of EM for the same incubation interval (Fig. 6c). The marine strains also showed stable biofilm adhesion levels when comparing 24-h to 48-h incubation intervals, whereas the reference strain exhibited lower biofilm adhesion after 48 h for all HDPE weathering levels (Fig. S1). These results suggest distinct biofilm adhesion and stability strategies adopted by these bacteria. Differently from the reference strain, the wild isolates from sea sediment may have been in close contact with a great diversity of organic molecules occurring in their environment, among which microplastics (usually weathered) are reported as very frequent [2, 3, 16]. Despite this diversity, the concentration of natural organic molecules in the deep sea is usually low, as they are oligotrophic environments, which may privilege microbial species that are able to use different molecules as carbon and/or energy sources, with low metabolic activity and growth rates [40]. Our marine isolates were previously observed as presenting a wide metabolic ability to use an interesting diversity of carbon sources, like different mono- and disaccharides, and organic acids, usually at lower growth rates, comparing to reference strains (unpublished data). The results of the present study are in line with these previous observations since our marine isolates efficiently attached weathered and non-weathered HDPE fragments but at lower rates when compared to the reference strain at 24 h of incubation. These marine strains exhibited lower biomass, with an observable efficient production of EM in 24-h biofilms. Therefore, the presence of extracellular polymeric substances on the EM could have provided mechanical stability for bacterial isolates on weathered surfaces [41], as an adaption to form stable long-term biofilms in different polymeric surfaces, which they can eventually use as carbon source as well [3]. This may explain the overall lower impact of HDPE weathering on the attachment of marine strain biofilms. As the reference strain is adapted to grow in artificial media and to form biofilms in non-weathered surfaces, as those we used in biofilms experiments, our data showed that this strain seemed to favor quicker cell division, with apparent low production of EM, resulting in larger biofilm biomass in non-weathered surfaces at the first 24 h of incubation.

By imaging biofilm structures, we also identified cell-cell and cell-surface attachment through extracellular appendages resembling *pili* structures [36, 42]. When these appendages occur in biofilms, they can be involved in the reversible attachment to abiotic or biotic surfaces, motility, and biofilm formation [36, 43]. We did not investigate which type of appendage they are, but different *pili*-like structures are reported as occurring in mature biofilm bacteria, facilitating intercellular interaction through aggregation or microcolony formation [7, 36]. Interestingly, there are no previous reports on *Lysinibacillus* sp. appendages involved in biofilm production on plastics. Thus, our SEM data of *Lysinibacillus* sp. M4 strain is likely the first indication that this genus might display this ability.

The biofilm formation data raised in this study corroborates the ability of *Pseudomonas* sp. strains from deep-sea sediment to adhere and efficiently form biofilms on plastic surfaces [44, 45]. Moreover, our *Pseudomonas* isolates showed to form a distinct clade in the phylogenetic tree, which may indicate they may represent undescribed strains of *P. rhodesiae* or even novel species of the *Pseudomonas fluorescens* group. Thus, they may also present undescribed metabolic properties to be explored.

Unlike several in vitro biofilm protocols [46, 47], our experiments were produced without a pre-induction of biofilm formation, thus highlighting the attachment efficiency of these marine isolates under experimental conditions. Moreover, our ATR-FTIR analysis suggested that these biofilms impact the chemical structure of HDPE fragments (Fig. 6a and b), reducing C–H stretching and increasing CH_2 bend absorbance in biofilm-colonized surfaces. Thus, these strains may be involved in the first steps of HDPE biodegradation, including fragments with increased roughness due to previous abiotic weathering.

As previously reported, seafloor currents operate in the transport and accumulation of microplastics over the seabed, creating microplastic hotspots in the oceans' sediment. Moreover, sequestration and burial of microplastics in sediment were also inferred as possible, under certain environmental conditions [16]. The microbes here analyzed displayed a clear potential regarding the biodegradation of plastic components, which may indicate signs of adaption to plastic contaminants. Therefore, our study contributes toward the biotechnological application of bacterial strains from deep-sea environments, reinforcing the need for further exploration of marine microbes with bioremediation potential.

Supplementary Information The online version contains supplementary material available at https://doi.org/10.1007/s00248-020-01666-8.

Acknowledgments We thank Petróleo Brasileiro S.A. (PETROBRAS) for collecting the samples and financial support; Indústria Petroquímica Braskem S.A. for proving HDPE pellets; the Central Laboratory of Microscopy and Microanalysis (LabCEMM/PUCRS) for preparing and assisting the microscopic visualization; CNPq (Brazilian National Council for Scientific and Technological Development) and Coordenação de Aperfeiçoamento de Pessoal de Nível Superior (Brasil) for the scholarships of master's students.

Funding The financial support was provided by Conegás II Project (PETROBRAS TC N° 0050.0096017.15.9) and IPR/PUCRS Research Fund. Funding was also provided by the Coordenação de Aperfeiçoamento de Pessoal de Nível Superior – Brasil (CAPES - Finance Code 001) and Brazilian National Council for Scientific and Technological Development (CNPq - master's scholarship).

Compliance with Ethical Standards

Conflict of Interest The authors declare they have no conflict of interest.

References

1. Wit W De, Hamilton A, Scheer R et al (2019) Por solucionar a poluição plástica: Transparência e responsabilização
2. Jambeck JR, Geyer R, Wilcox C et al (2015) Plastic waste inputs from land into the ocean
3. Jacquin J, Cheng J, Odobel C, Pandin C, Conan P, Pujo-Pay M, Barbe V, Meistertzheim AL, Ghiglione JF (2019) Microbial ecotoxicology of marine plastic debris: a review on colonization and biodegradation by the "plastisphere.". Front Microbiol 10. https://doi.org/10.3389/fmicb.2019.00865
4. Keswani A, Oliver DM, Gutierrez T, Quilliam RS (2016) Microbial hitchhikers on marine plastic debris: human exposure risks at bathing waters and beach environments. Mar Environ Res 118:10–19. https://doi.org/10.1016/j.marenvres.2016.04.006
5. Rummel CD, Jahnke A, Gorokhova E, Kühnel D, Schmitt-Jansen M (2017) Impacts of biofilm formation on the fate and potential effects of microplastic in the aquatic environment. Environ Sci Technol Lett 4:258–267. https://doi.org/10.1021/acs.estlett.7b00164
6. Lohse MB, Gulati M, Johnson AD, Nobile CJ (2018) Development and regulation of single-and multi-species *Candida albicans* biofilms. Nat Rev Microbiol 16:19–31. https://doi.org/10.1038/nrmicro.2017.107
7. Flemming HC, Wingender J, Szewzyk U, Steinberg P, Rice SA, Kjelleberg S (2016) Biofilms: an emergent form of bacterial life. Nat Rev Microbiol 14:563–575. https://doi.org/10.1038/nrmicro.2016.94
8. UNEP (2016) Marine plastic debris and microplastics – global lessons and research to inspire action and guide policy change. United Nations Environ Program
9. Coutinho FMB, Mello IL, de Santa Maria LC (2003) Polietileno: principais tipos, propriedades e aplicações. Polímeros 13:01–13. https://doi.org/10.1590/S0104-14282003000100005
10. Mohsenzadeh A, Zamani A, Taherzadeh MJ (2017) Bioethylene production from ethanol: a review and techno-economical evaluation. ChemBioEng Rev 2:75–91
11. Da Luz JMR, Paes SA, Ribeiro KVG et al (2015) Degradation of green polyethylene by *Pleurotus ostreatus*. PLoS One 10. https://doi.org/10.1371/journal.pone.0126047
12. Shah AA, Hasan F, Hameed A, Ahmed S (2008) Biological degradation of plastics: a comprehensive review. Biotechnol Adv 26:246–265. https://doi.org/10.1016/j.biotechadv.2007.12.005
13. Thompson RC, Olson Y, Mitchell RP et al (2004) Lost at sea: where is all the plastic? Science (80-) 304:838. https://doi.org/10.1126/science.1094559
14. Koelmans AA, Kooi M, Law K, Van Sebille E (2017) All is not lost: fragmentation of plastic at sea. Environ Res Lett 12:114028
15. Choy CA, Robison BH, Gagne TO et al (2019) The vertical distribution and biological transport of marine microplastics across the epipelagic and mesopelagic water column. Sci Rep 9:7843. https://doi.org/10.1038/s41598-019-44117-2
16. Kane IA, Clare MA, Miramontes E et al (2020) Seafloor microplastic hotspots controlle by deep-sea circulation. Science (80-) 368:1140–1145. https://doi.org/10.1126/science.aba5899
17. Pathak VM, Navneet (2017) Review on the current status of polymer degradation: a microbial approach. Bioresour Bioprocess 4. https://doi.org/10.1186/s40643-017-0145-9
18. Lobelle D, Cunliffe M (2011) Early microbial biofilm formation on marine plastic debris. Mar Pollut Bull 62:197–200. https://doi.org/10.1016/j.marpolbul.2010.10.013
19. Harshvardhan K, Jha B (2013) Biodegradation of low-density polyethylene by marine bacteria from pelagic waters, Arabian Sea, India. Mar Pollut Bull 77:100–106. https://doi.org/10.1016/j.marpolbul.2013.10.025
20. Zettler ER, Mincer TJ, Amaral-Zettler LA (2013) Life in the "plastisphere": microbial communities on plastic marine debris. Environ Sci Technol 47:7137–7146. https://doi.org/10.1021/es401288x
21. Morohoshi T, Oi T, Aiso H, Suzuki T, Okura T, Sato S (2018) Biofilm formation and degradation of commercially available biodegradable plastic films by bacterial consortiums in freshwater environments. Microbes Environ 00:0–3. https://doi.org/10.1264/jsme2.ME18033
22. Miller DJ, Ketzer JM, Viana AR, Kowsmann RO, Freire AFM, Oreiro SG, Augustin AH, Lourega RV, Rodrigues LF, Heemann R, Preissler AG, Machado CX, Sbrissa GF (2015) Natural gas hydrates in the Rio Grande Cone (Brazil): a new province in the western South Atlantic. Mar Pet Geol 67:187–196. https://doi.org/10.1016/j.marpetgeo.2015.05.012
23. Giongo A, Haag T, Simão TLL, Medina-Silva R, Utz LRP, Bogo MR, Bonatto SL, Zamberlan PM, Augustin AH, Lourega RV, Rodrigues LF, Sbrissa GF, Kowsmann RO, Freire AFM, Miller DJ, Viana AR, Ketzer JMM, Eizirik E (2016) Discovery of a chemosynthesis-based community in the western South Atlantic Ocean. Deep Res Part I Oceanogr Res Pap 112:45–56. https://doi.org/10.1016/j.dsr.2015.10.010
24. Harrison JJ, Turner RJ, Ceri H (2005) Persister cells, the biofilm matrix and tolerance to metal cations in biofilm and planktonic *Pseudomonas aeruginosa*. Environ Microbiol 7:981–994. https://doi.org/10.1111/j.1462-2920.2005.00777.x
25. Edwards U, Rogall T, Blöcker H, Emde M, Böttger EC (1989) Isolation and direct complete nucleotide determination of entire genes. Characterization of a gene coding for 16S ribosomal RNA. Nucleic Acids Res 17:7843–7853. https://doi.org/10.1093/nar/17.19.7843
26. Kumar S, Stecher G, Li M, Knyaz C, Tamura K (2018) MEGA X: molecular evolutionary genetics analysis across computing platforms. Mol Biol Evol 35:1547–1549. https://doi.org/10.1093/molbev/msy096
27. Tamura K, Nei M (1993) Estimation of the number of nucleotide substitutions in the control region of mitochondrial DNA in humans and chimpanzees. Mol Biol Evol 10. https://doi.org/10.1093/oxfordjournals.molbev.a040023
28. Q-Lab (2018) QUV Accelerated Weathering Tester. https://www.q-lab.com/products/quv-weathering-tester/quv#videos. Accessed April 2020
29. Moore CJ, Moore SL, Leecaster MK, Weisberg SB (2001) A comparison of plastic and plankton in the North Pacific Central Gyre. Mar Po 42:1297–1300
30. Chari PVB, Viswadeepika K, Kumar BA (2014) In vitro biofilm forming capacity on abiotic contact surfaces by outbreak-associated *Vibrio harveyi* strains. J Coast Life Med 2:132–140. https://doi.org/10.12980/JCLM.2.2014B85
31. Stepanović S, Ćirković I, Ranin L, Švabić-Vlahović M (2004) Biofilm formation by *Salmonella* spp. and *Listeria monocytogenes* on plastic surface. Lett Appl Microbiol 38:428–432. https://doi.org/10.1111/j.1472-765X.2004.01513.x
32. Bhushan B (2000) Surface roughness analysis and measurement techniques. In: Modern tribology handbook: volume one: principles of tribology. pp 49–119
33. Rajesh Kumar B, Subba Rao T (2012) AFM studies on surface morphology, topography and texture of nanostructured zinc aluminum oxide thin films. Dig J Nanomater Biostruct 7:1881–1889

34. Almond J, Sugumaar P, Wenzel MN, Hill G, Wallis C (2020) Determination of the carbonyl index of polyethylene and polypropylene using specified area under band methodology with ATR-FTIR spectroscopy. E-Polymers 20:369–381. https://doi.org/10.1515/epoly-2020-0041
35. Zerbi G, Gallino G, Del Fanti N, Baini L (1989) Structural depth profiling in polyethylene films by multiple internal reflection infrared spectroscopy. Polymer (Guildf) 30:2324–2327. https://doi.org/10.1016/0032-3861(89)90269-3
36. Berne C, Ducret A, Hardy GG, Brun YV (2015) Adhesins involved in the attachment to abiotic surfaces by Gram-negative bacteria. Microbiol Spectr 3:1–45. https://doi.org/10.1128/microbiolspec.MB-0018-2015.Adhesins
37. Jung MR, Horgen FD, Orski SV, Rodriguez C. V, Beers KL, Balazs GH, Jones TT, Work TM, Brignac KC, Royer SJ, Hyrenbach KD, Jensen BA, Lynch JM (2018) Validation of ATR FT-IR to identify polymers of plastic marine debris, including those ingested by marine organisms. Mar Pollut Bull 127:704–716. https://doi.org/10.1016/j.marpolbul.2017.12.061
38. Esmaeili A, Pourbabaee AA, Alikhani HA et al (2013) Biodegradation of low-density polyethylene (LDPE) by mixed culture of *Lysinibacillus xylanilyticus* and *Aspergillus niger* in soil. PLoS One 8. https://doi.org/10.1371/journal.pone.0071720
39. Andy M. Booth, Stephan Kubowicz, CJ Beegle-Krause, Jørgen Skancke, Tor Nordam, Eva Landsem M, Throne-Holst SJ (2018) Microplastic in global and Norwegian marine environments: Distributions, degradation mechanisms and transport
40. Hoehler TM, Jørgensen BB (2013) Microbial life under extreme energy limitation. Nat Rev Microbiol 11:83–94. https://doi.org/10.1038/nrmicro2939
41. Flemming HC, Wingender J (2010) The biofilm matrix. Nat Rev Microbiol 8:623–633. https://doi.org/10.1038/nrmicro2415
42. Tomaras AP, Dorsey CW, Edelmann RE, Actis LA (2003) Attachment to and biofilm formation on abiotic surfaces by *Acinetobacter baumannii*: involvement of a novel chaperone-usher pili assembly system. Microbiology 149:3473–3484. https://doi.org/10.1099/mic.0.26541-0
43. Toyofuku M, Inaba T, Kiyokawa T, Obana N, Yawata Y, Nomura N (2016) Environmental factors that shape biofilm formation. Biosci Biotechnol Biochem 80:7–12. https://doi.org/10.1080/09168451.2015.1058701
44. Kyaw BM, Champakalakshmi R, Sakharkar MK, Lim CS, Sakharkar KR (2011) Biodegradation of low density polythene (LDPE) by *Pseudomonas* species. Indian J Microbiol 52:411–419. https://doi.org/10.1007/s12088-012-0250-6
45. Esmaeili A, Pourbabaee AA, Alikhani HA, Shabani F, Kumar L (2014) Colonization and biodegradation of photo-oxidized low-density polyethylene (LDPE) by new strains of *Aspergillus* sp. and *Lysinibacillus* sp. Bioremediat J 18:213–226. https://doi.org/10.1080/10889868.2014.917269
46. O'Toole G, Kaplan HB, Kolter R (2000) Biofilm formation as microbial development. Annu Rev Microbiol 54:49–79. https://doi.org/10.1146/annurev.micro.54.1.49
47. Ibarra-Trujillo C, Villar-Vidal M, Gaitán-Cepeda LA, Pozos-Guillen A et al (2012) Formation and quantification assay of *Candida albicans* and *Staphylococcus aureus* mixed biofilm. Rev Iberoam Micol 29:214–222. https://doi.org/10.1016/j.riam.2012.02.003